

Application of the Acoustic Emission Technique for Damage Identification in the Fiber Reinforced Polymer Composites

Sylwester Samborski^{1*}, Izabela Korzec¹

¹ Lublin University of Technology, 36 Nadbystrzycka St., 20-618 Lublin, Poland

* Corresponding author's e-mail: s.samborski@pollub.pl

ABSTRACT

A set of experiments having in target determination of fracture resistance was performed on the Fiber Reinforced Polymer (FRP) composites specimens with an additional monitoring of damage onset and evolution with a so-called Acoustic Emission (AE) technique. The AE technique is a non-destructive material testing method, which enables registering the phenomena usually not audible with a human ear – the frequency bands lay between 100 and 1000 kHz. For the FRP composites this enables monitoring various damage phenomena – matrix cracking, delamination, fiber cracking etc. by acquisition and subsequent analysis of several AE parameters: number of hits, number of counts, amplitude or energy of the signal. In the paper advantages of a deeper analysis of the raw AE signal was presented with an application of the Fast Fourier Transform (FFT), leading to a more detailed damage identification along the whole loading procedure. The study proved the usability of the AE method in damage monitoring of the FRPs; a bundle of illustrative examples of chosen acoustic emission parameters' evolution displayed on the background of the load applied to composite specimens was presented and interpreted.

Keywords: damage, composite, acoustic emission, fast Fourier transform.

INTRODUCTION

The growing field of applications of laminate composites such as the Fiber Reinforced Polymer Composite (FRPC) in contemporary structures yields from their advantageous strength-to-mass ratio and the possibility of tailoring the mechanical characteristics mainly by specific layups [1, 2]. In the light of these tendencies, it reveals to be necessary to detect any damage in composite structures, starting from the production process along the whole period of maintenance of the machine parts made of laminates. Among many different damage identification techniques Acoustic Emission (AE) reveals its advantages, such as high sensitivity, ability to monitor the structures during their normal operation, location of the damage source in real time by using several piezoelectric sensors etc. [3]. The most important virtue of the AE is ability to detect damage phenomena that cannot be heard nor seen by human

senses. Occurrence like damage was described in details by Kubiak and others. Authors focused on destruction phenomena taking place in a composite the results showed different value of frequency: lower value of frequency till 200 kHz reflected separation of plies, above of 300 kHz was related to fibre pull-out. The frequencies upper 400 kHz described breaking fibres [4]. As it is shown further in this article, a detailed analysis of full AE signal, for example with Fast Fourier Transform (FFT) enables identification of different types of defects during their occurrence [5]. FRP composites become more and more widely used in a range of industry, that's why the monitoring of its damage is also necessary. Acoustic emission (AE) enables non-destructive (NDT) monitoring of damage initiation and development in an engineering materials. Compared to other NDT methods, acoustic emission is use during experimental tests while other methods are used before or after loading [6]. Damage in FRP composites can have

a form of localized or distributed devastation throughout the material space. As an example, distributed damage due to fatigue can be found in a lot of works. Nonetheless, there are also few publications on the use of AE for quantitative estimation of fatigue damage [7]. Leone and others confirmed that number of emissions at failure was dependent on the residual strength where specimens exhibiting a higher strength and in the same time showed a higher AE activity. This phenomena indicate that some usefull information about the material residual strength is in the trend of the AE curves [8].

THEORETICAL FUNDAMENTALS OF ACOUSTIC EMISSION AND THE FAST FOURIER TRANSFORM

The term “acoustic emission” is somewhat misleading, as the human ear audible range does not exceed 20 kHz (typically 1–4kHz concerning speech [9]) while the AE frequencies are 100 kHz – 1 MHz for standard applications. In contemporary industry the acoustic emission monitoring installations are used in non-destructive testing of highly loaded machine parts made of the FRPCs (airplanes, boats, gas tanks etc.) [10, 11, 12] inspection of welds, high-voltage discharges or seismic research. The founding phenomenon exploited in the acoustic emission technology is elastic wave propagation in solids experiencing sudden release of the accumulated strain energy [3, 10].

As to the authors’ experience in the acoustic emission monitoring of damage phenomena in laminated composites [12, 13, 14], the raw continuous AE signal can be parameterized by catching its changes in the form of counts (number of threshold crossings) and hits, i.e. the damage events. These two are the classical AE measures. Other parameters describing the phenomena of elastic energy release are the amplitude, the energy, or the Root-Mean-Square (RMS) value of the raw AE signal [3]. Note, there is a relation between the cumulative number of hits and the fracture toughness, i.e. the resistance to delamination growth. The same applies to the AE signal amplitude [15, 16].

The Vallen’s AMSY 5 acoustic emission hardware and the dedicated software allows a profound analysis of the raw AE signal – among others, by application of the FFT procedure,

which leads to distinction of different damage phenomena, together with their sequence in time of the experiment. Usually, in composite materials there are three dominating frequency bands: 60–150 kHz, 200–300 kHz and 400–500 kHz [5, 14]. The bands listed above can be identified with matrix cracking, interlaminar crack propagation (delamination) with fiber pull out, as well as the fiber cracking, respectively. Concerning the process of delamination itself, the frequencies around 200 kHz reveal the cleavage of the neighboring plies in macroscopic sense, whereas those approaching 300 kHz occur during fiber pull-out, for example in the DCB tests, when the bridging phenomenon takes place.

The Fast Fourier Transform is a way to calculate quickly the Discrete Fourier Transform (DFT) of a signal time series. In the case of the raw AE data, the FFT enables getting the frequency spectra for any given moment of the experiment and as such helps to reveal the defect type when related to the load downcast and the other AE parameters. There are many algorithms to calculate the FFT today. In any case, the vibration signal – the elastic wave induced by a defect, given in time domain as real numbers is transformed to the complex sequence in the frequency domain.

Typically, the FFT can be computed with the formula provided by Cooley and Tukey [17]:

$$X(f) = \sum_{n=0}^{N-1} x(n) e^{-i2\pi n f / N} \quad (1)$$

where: $x(n)$ is the amplitude of the discretized signal (in time domain) and X is the resulting height of the FFT peak for any of the n -th discrete frequencies f ;

i is the imaginary unit. Note, that the sampling frequency in the AE measurements performed by the authors during the experiments was 10MHz and the number of samples in any of the wavelets was $2^{10}=1024$.

Recently application of the acoustic emission sensors has been found useful by some authors from the point of view of more precise determination of propagation initiation [5, 15, 19]. This is however not the object of the current paper, as it aims at identification of the specific damage phenomena taking place in the deformed composite specimen and as such tends to look forward into

the area of damage identification in composites using the modern AE facilities. As mentioned above, this goal can be achieved through a detailed FFT analysis of the raw AE signal, aside from the classical parameters (hits and counts). The analysis presented further in this article covers chosen specimens from the ENF tests performed by the authors. The specimens differed with the laminate sequence and – in particular – they had various mis-orientation of fiber directions in the very inter-layer of delamination (cf. the paper by Pereira and de Morais [12]).

MATERIALS AND METHODS

The acoustic emission signal acquisition system used in the experiments was the Vallen's "AMSY", version 5 [3]. The commonly used piezoelectric sensors are the most appropriate for AE tests, due to their sensitivity within the typical range of the acoustic emission frequencies. Typically, the sensor is attached to a specimen through a clamp, glue, magnetic holder etc. In the case of the experiments performed by the authors, a silicone grease and an elastic clamp were used together (Fig. 1), in order to provide both stable attachment of the FUJICERA 1045S (range 200 – 1300kHz) sensor to the composite beam specimen and the best signal conductance.

The next element in the AE measurement chain was the AEP4 pre-amplifier (noise threshold of 34dB), which strengthened the sensor's signal and transmitted it to the ASIP-2 data conversion card (A/D, 40MHz sampling frequency, 18-bit resolution, band width 1.6 kHz – 2.4 MHz).

System AMSY-5 was used to register acoustic emission parameters (Fig. 2). The data was collected on computer's hard drive. The last step was applied to conduct the analysis by a software.

In order to synchronize the acoustic emission results in time with the load and deformation of the composite specimens, the axial force induced by the Shimadzu AGS-X (Fig. 3) universal testing machine was gathered in real time from its load cell and registered in the AE computer, among other results. Later, on the background of the load, all the acoustic results could be synchronized with the specimens' deformation and thus the subsequent damage phenomena were recognized by the frequency analysis.

RESULTS AND DISCUSSION

The acoustic emission results were registered during the end-notched flexure (ENF) tests performed on laminated composite beam specimens. As it is explained in the respective ASTM Standard [18] the specimen must be bent in a three-point bending (3PB) apparatus. During the whole test, a permanent registration of the loading force, the displacement and the actual crack (delamination) length must be lead.

In Figure 4 the load curve is a background for the AE signal energy for the ENF specimen having a 30°// -30° delamination interface.

In the analysis of the AE results for a number of the ENF specimens it turned out, that a good indicator of the very beginning (the onset) of delamination propagation was the plot of energy (see Fig. 4), in which the peaks occurred slightly

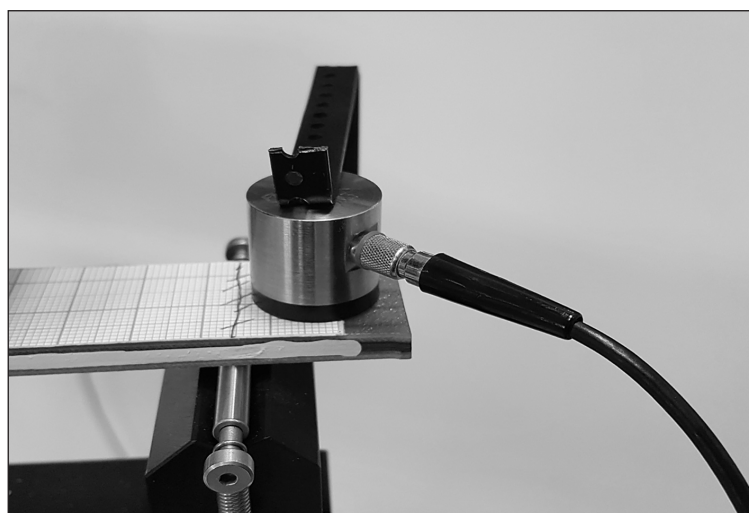


Figure 1. An ENF composite specimen with AE sensor

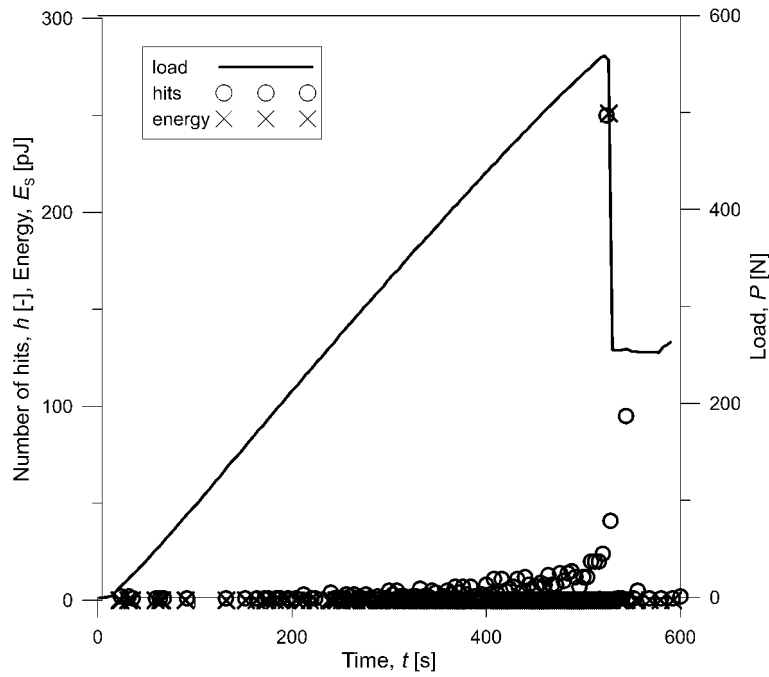


Fig. 2. System AMSY-5

before the very moment of the load deviation from linearity. In accordance to the results of Ducept et al. [20] it proved the sensitivity of the AE technique, which detected the damage onset earlier than any classical method – the P_{max} , the 5 % or the NL one. This finding is significant from the point of view of getting the very beginning

of delamination growth and can be utilized while computing the initiation fracture toughness (G_{IIC} in case of the ENF tests). However, as mentioned above, the current paper has in target deeper analysis of the raw AE signal, for which the onset of damage is only the beginning and the research covers the whole process of delamination

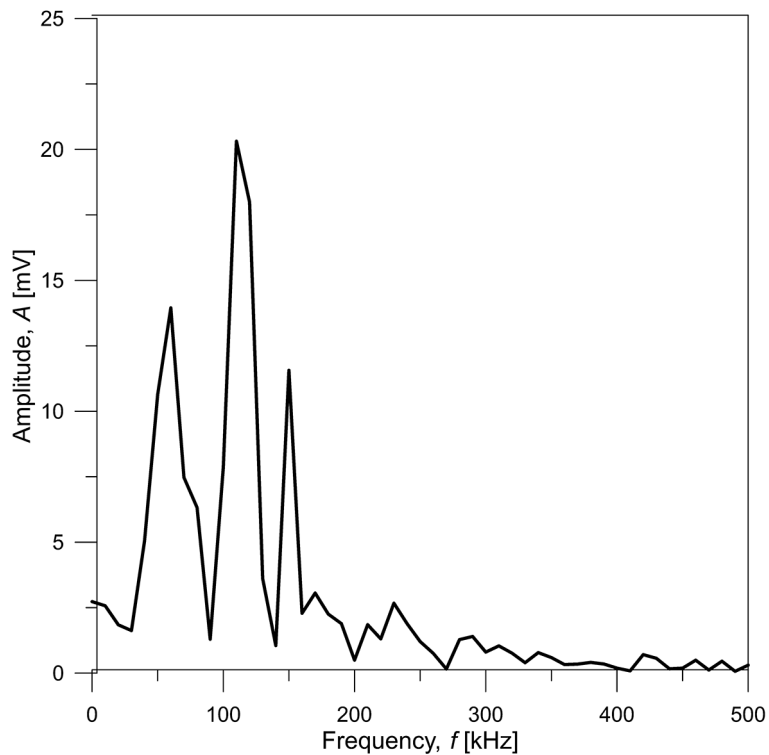


Fig. 3. Tensile test configuration with an instrumented composite specimen

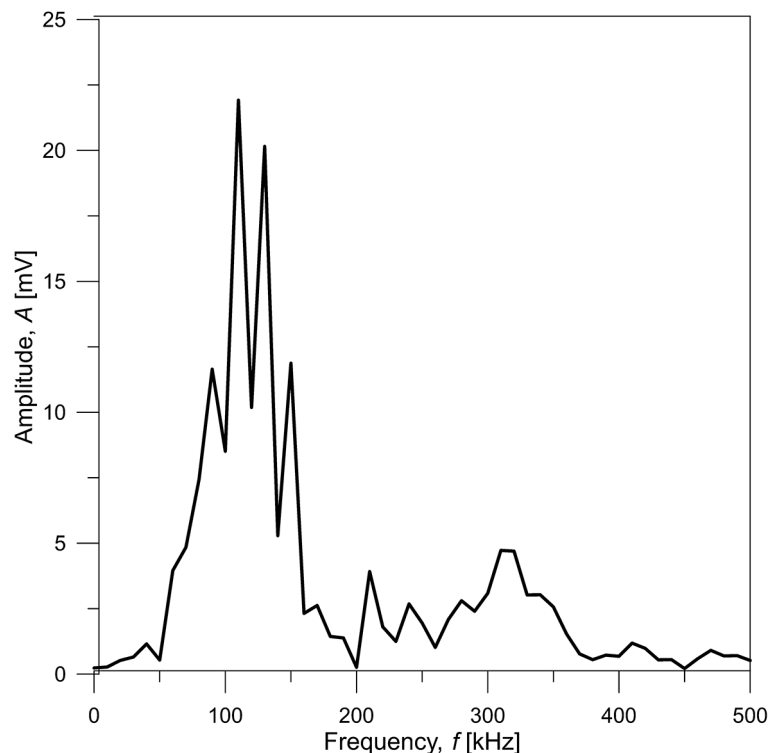


Figure 4. Acoustic emission data on the background of the axial load applied to an ENF composite specimen

propagation until the very end of the test, during which the identification of different damage phenomena can be performed. Thus, in the next paragraphs there are the figures with the frequency spectra and the comments on the forms of damage revealed in the end of the tests.

The first specimen under consideration was the one with the $30^\circ//30^\circ$ interface, for which the load vs time plot nonlinearity started around 650th second of the test; the maximal load occurred in the 746th second. The FFT plots for the two time points and the interval between them revealed the AE signal frequencies within the range of 60–150 kHz (Fig. 5), typical for the polymer matrix cracking. This fact is in agreement with the delamination phenomenon observed visually in the ENF test at the respective time. While the test approached to its end and the final failure process began, an intensive increase in the number of hits and counts was observed the frequency peaks moved towards the band of 100–300 kHz, revealing the macroscopic cleavage of the composite specimen and the fiber pull-out.

The two subsequent figures (Fig. 6 and Fig. 7) show the FFT for the symmetric and anti-symmetric delamination interface at a bigger fiber angle equal 60 degrees. For the $60^\circ//60^\circ$ -interface specimen (Fig. 6), beside the high peaks in the 90–150 kHz range (matrix cracking) one

can note a peak at 215 kHz (macro-cleavage) and another one around 320 kHz (fiber pull-out). The peaks are shifted to the left for the $60^\circ//60^\circ$ case: 80–130 kHz, 200 kHz and 250 kHz, respectively. These observations apply to the delamination onset moment and suggest an influence of the mutual mis-orientation of the reinforcement fibers in the neighboring composite layers. Namely, in the symmetric case the fibers were aligned, whereas in the antisymmetric one they were crossed at an angle of 60° . It seems obvious, that in the latter case the energy needed to induce any kind of damage in the composite should be lower because of weaker bonding between the crossed fibers [21] and thus the FFT peaks occur at slightly lower frequencies. This is however a hypothesis which could be confirmed in further experiments including fractographic analysis [15, 22, 23]. In comparison to the smaller interface-angle specimen ($30^\circ//30^\circ$), the FFT spectrum was however moved right, which leads to another finding, saying that the value of the fiber angle itself can also affect the frequencies of the elastic waves emitted by particular kinds of damage. The additional clue for this is, that at the end of the test, when the catastrophic failure runs, the “60 degree” specimens exhibit the FFT peaks practically only at 130–140 kHz; the higher frequencies of ca. 250 kHz come out only

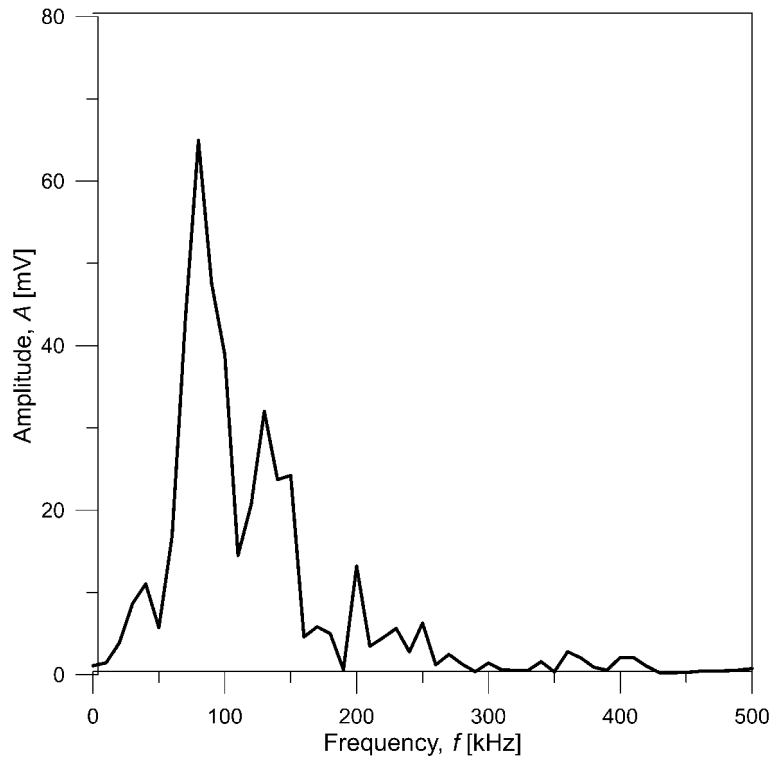


Figure 5. Frequency spectrum of the composite specimen with the 30°//−30° delamination interface

occasionally during the failure process. This can be acknowledged as a preliminary confirmation of the above stated hypothesis on the weaker debonding energy for crossed neighboring fibers.

The last ENF case analyzed in the current study was the 90°//90° interface case (Fig. 8), in which the fibers are not crossed, but their direction is perpendicular to the specimen’s axis.

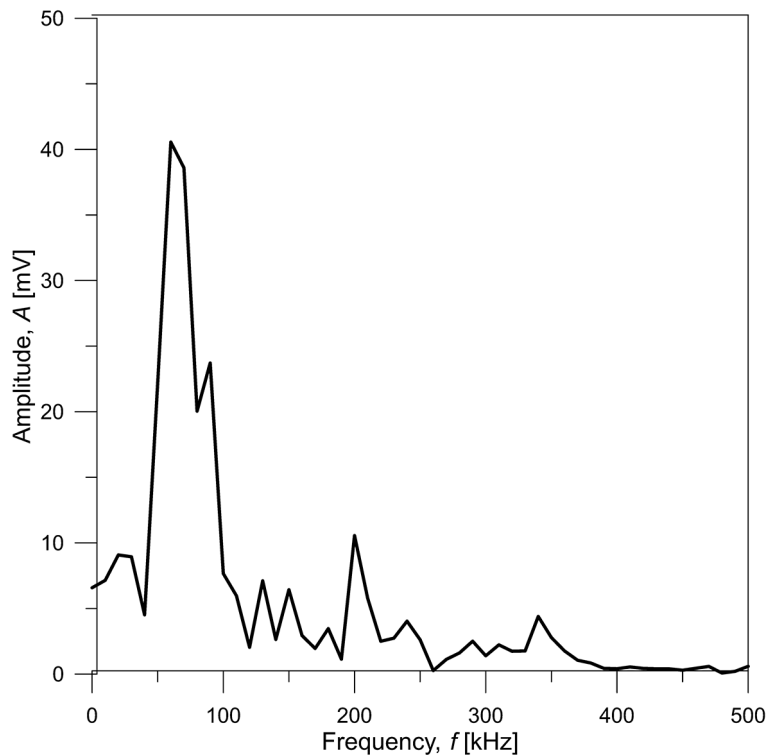


Figure 6. Frequency spectrum of the composite specimen with the 60°//60° delamination interface

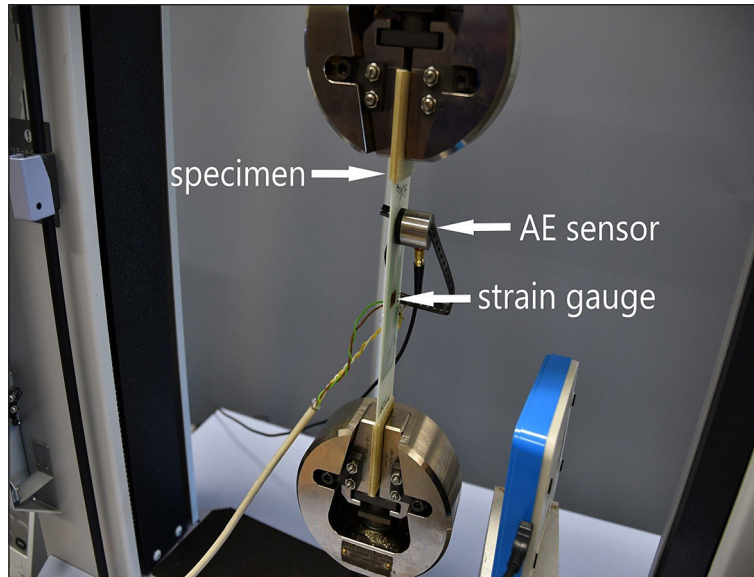


Figure 7. Frequency spectrum of the composite specimen with the 60°//60° delamination interface

There was only one big peak observed within the first frequency band, responsible for the matrix cracking. This can indicate a bit different damage mechanism of the “90 degree” layers, which can easily break between the fibers due to the low

strength of any FRPC composite in the direction perpendicular to the reinforcing fibers, when only the polymer matrix itself carries practically the whole load; it is reflected by relatively low frequency of the first peak – ca. 70 kHz. On the other

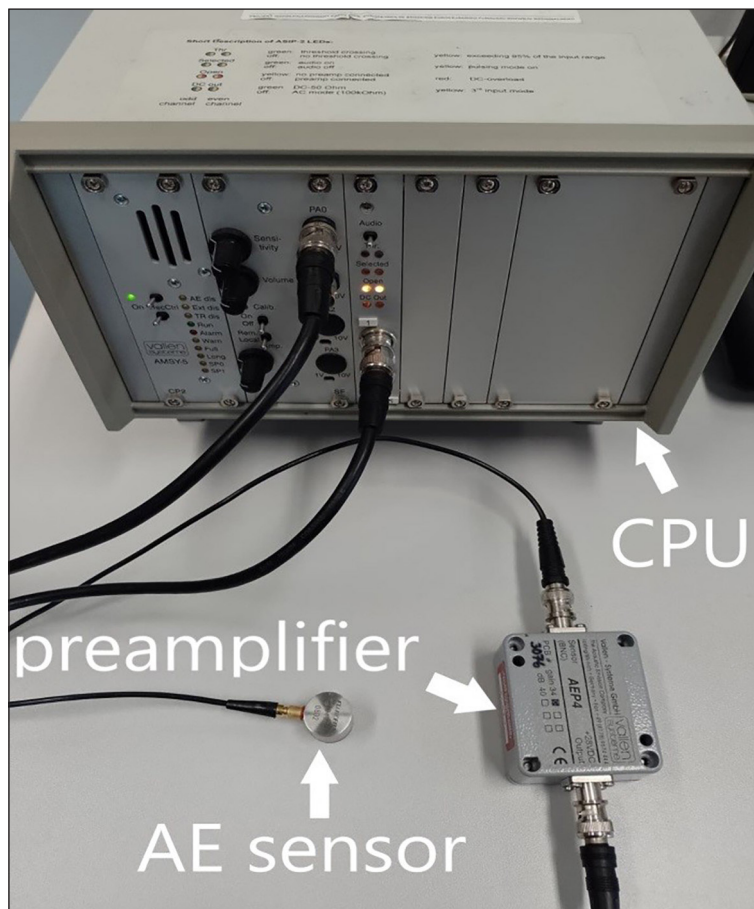


Figure 8. Frequency spectrum of the composite specimen with the 90°//90° delamination interface

hand, the rest of the frequency spectrum reflects a typical macroscopic delamination process with two main peaks at 200 kHz and 340 kHz.

At the end of the current section it is worth underlining, that in the performed 3PB (ENF) tests practically no fiber cracking was observed, even in the end of the tests. This was obviously connected to the loading configuration and the nature of the ENF test, which did not favor sudden nor catastrophic deformation of the composite specimen, as it was observed, for example in buckling [24] or tension experiments. The AE analyses performed by the authors during the compressive tests of composite profiles [11, 16, 20] revealed the FFT peaks at ca. 400 kHz proving the intensive fiber cracking during final failure.

To better present and compare AE method there have been made similar specimens to describe their similarities and discrepancies of selected acoustic emission parameters recorded during tensile tests of fiber reinforced composite specimens, made of glass-fabric/epoxy prepreg (VTC401-C200T-T300–2X2T-3K-42%RW produced by SHD Composite Materials Ltd.) with the autoclaving method. The orientation of the

fabric layers were 0°/90° degree. The resin were mixed in a ratio 100:40 by using L285 resin and MGS hardener. Basic properties of the prepreg were: fiber volume fraction equal 50–60%, strain to failure 1.7 %, flexural strength 863 MPa, tensile strength 573 MPa. The tests were carried out at 23±2°C and 50±5% RH. Main dimensions of the specimens are collected in Table 1. The samples are not identical, although they are made very precisely (the same width shown good quality of the samples and the milling technique). Less accurate is the thickness, because the autoclaving process is more difficult to control.

The four examples were chosen intentionally to display both similarities of the AE results for glass specimens of the same kind and to discuss apparent differences in time courses of the acoustic parameters within the group of samples. The presented results show advantages of AE monitoring of destructive tests, such as detecting any premature damage in a specimen and – above all – precise indication of the onset of its final failure with the corresponding maximal load, used in further calculations of strength or fracture toughness.

Table 1. Geometrical parameters of the composite specimens tested in tension

Sample series	Width, <i>B</i> [mm]	Thickness, <i>H</i> [mm]	Length, <i>L</i> [mm]
S1	36.52	1.18	250.00
S2	36.52	1.18	250.00
S3	36.52	1.16	250.00
S4	36.52	1.18	250.00

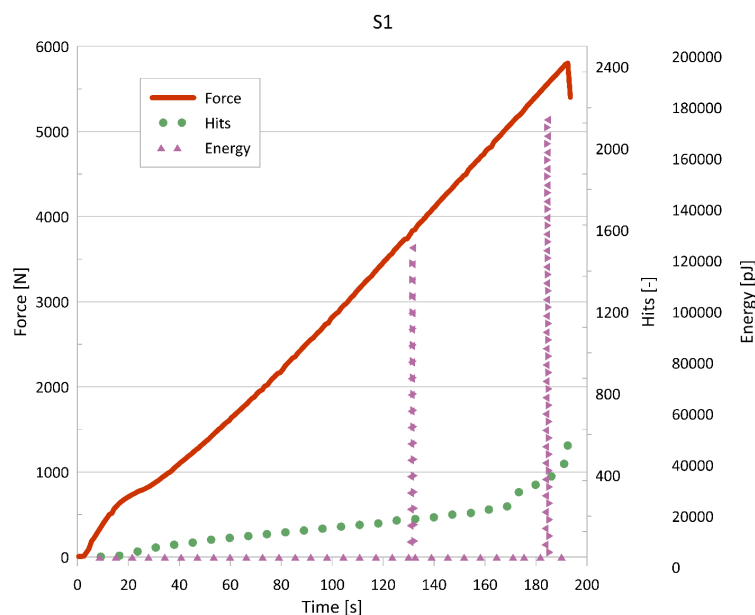


Figure 9. Acoustic emission results on the background of the load applied to specimen S1

The first graph (Fig. 9), elaborated for the specimen S1 shows time course of the loading force during tensile strength test as a background of acoustic emission parameters (released along with damage evolution): hits and energy, in the form of cumulated plots. The cumulative form of the graphs makes it easier to conclude on specimen deterioration, intensity of which is naturally higher right before final failure. The noticeable nonlinearity of the force diagram in the initial loading phase was a typical phenomenon in any experiment; it was due to the clearance canceling of the machine clamps, while gripping the specimen etc. During this process one can noticed small increments in the number of hits (damage events), but the AE energy peaks were virtually absent at that time. It means that in the initial phase of the specimen’s forced elongation no damage occurred. Next, above 1000 N and up to the maximal (failure) load, the force diagram was practically linear, with an abrupt ending; this indicates the onset of brittle – unstable, catastrophic fracture. It can also be concluded that small fluctuations in force values within the range of 2–3 kN were not associated with any important development of damage, because there were no energy peaks and the plot of cumulative number of hits was monotonic; the FFT analysis at that stage of the experiment gave frequencies from 70 to 100 kHz, typical for matrix cracking. Wevers and others also got similar results of damage in a range of matrix cracking [6]. On the other hand,

in the vicinity of the specimen’s failure the intensity of cracking process was indicated by rapid increase in the number of hits – between the 169th and the 194th second of the test, i.e. from the 584th to the 1404th damage event). The dominating AE frequency at that point was 320 kHz.

The next graph, gained for the sample S2, also shown some nonlinearity in the initial phase of the tensile test, with even less increments in the number of hits and energy, but in the range of force values of 1200–4000 N it was linear. The slight initial degradation of the material that took place at 106th second preceded two small energy peaks around the 109th and the 121th second, corresponding to various frequencies of the elastic wave released in the material: 50, 100 and 300 kHz. Kubiak et al. obtained similar frequency results, thus described the consequences of defects [4] In general, the former two values indicate matrix cracking, while the latter high frequency reveals fiber cracking [9] which is natural in the final phase of the destructive tension test. One can see an explicit increase in the number of damage events (hits) between the 2nd and 3rd energy peak; it is possible that occur intra-layer failure in a 114th – 117th s it was given 300 kH. In general, the former two values indicate matrix cracking, while the latter high frequency reveals fiber cracking [9] which is natural in the final phase of the destructive tension test. One can see an explicit increase in the number of damage events (hits) between the 2nd and 3rd energy peak; it is possible that

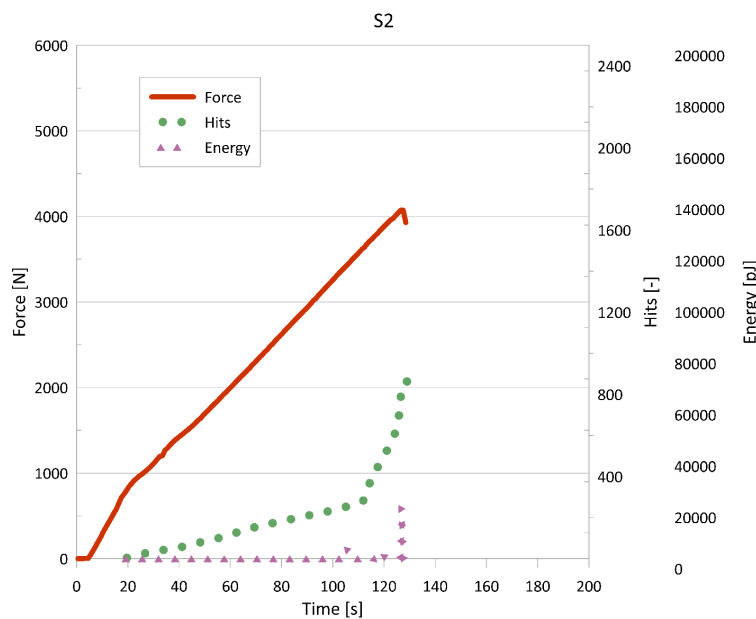


Figure 10. Acoustic emission results on the background of the load applied to specimen S2

an intensive fiber cracking took place between the 107th and 127th second, as the corresponding AE frequency (dominating) was ca. 300 kHz. The linearity of the force diagram was sustained until end – sharp drop of force at 127th second is again an indicative factor of brittle fracture. The value of the ultimate load was 4072.5 N, at the 4th peak of AE energy equal 134 pJ; the maximum number of hits at failure of the specimen S2 reached a plateau at 2082 increased from a value of 657 (at 111th second – between the two minor energy peaks) in a relatively short time interval of about 15 s. This reveals quite intensive damage evolution process. It is worth comparing the results with those of the specimen S1, where a relatively high energy peak at the 127th second of the test wasn't accompanied by any significant damage phenomena – monotonic increase in the number of hits (see Fig. 10), because it reveals possible discrepancies in experimental outcomes in one group of composite specimens.

The next graph (Fig. 11) shown a slightly different character of the hits curve for the specimen S3, even though the low energy peaks in the second half of the test remind the plots of the specimen S1. Namely, in the final phase of loading, the slope of the hits graph increased more smoothly than it was in a previous case (S2), where a clear “break” of the curve, making it somehow bi-linear was visible (Fig. 10). In the case of the current sample, the curvature of the hits plot was accompanied by only small energy peaks – about 100 pJ. At the same time, the last

energy peak had a small value, compared to the previous 2 samples (peak values), which indicated a less rapid cracking process in the specimen S3, although the force diagram had a sharp peak in the final phase. Above 1000 N, up to the maximal force, the diagram was linear (of course, excluding its initial section); the sharp drop in force after reaching 5120 N was indicative for brittle fracture of the material, as confirmed by the sharp increase in energy at the 165th second (hit 226) and a dramatic increase in the number of damage events between the 136th – 166th second (1025th – 2893th hit). In addition, a pronounced analysis of the raw AE signal revealed the frequencies of the elastic waves around 50 and 350 kHz. This again is an evidence of both matrix and reinforcement (fiber) cracking at the moment of the S3 specimen failure.

The last set of plots (Fig. 12), obtained for the specimen S4 contains the time course of the loading force in the tensile strength test. The force was growing linearly to its maximal value of 4328 N, after which the material failed, releasing a significant amount of elastic energy – the last peak reached 5343 pJ. The destruction was preceded by a rapid growth of the number of hits – from 701 to 2106. Again, the course of the latter part of the hits graph was typical for the considered group of specimen. However, the FFT analysis at the break point gave two main frequencies: 80 kHz for matrix cracking and quite high, but typical for brittle cracking for fibers – 470 kHz.

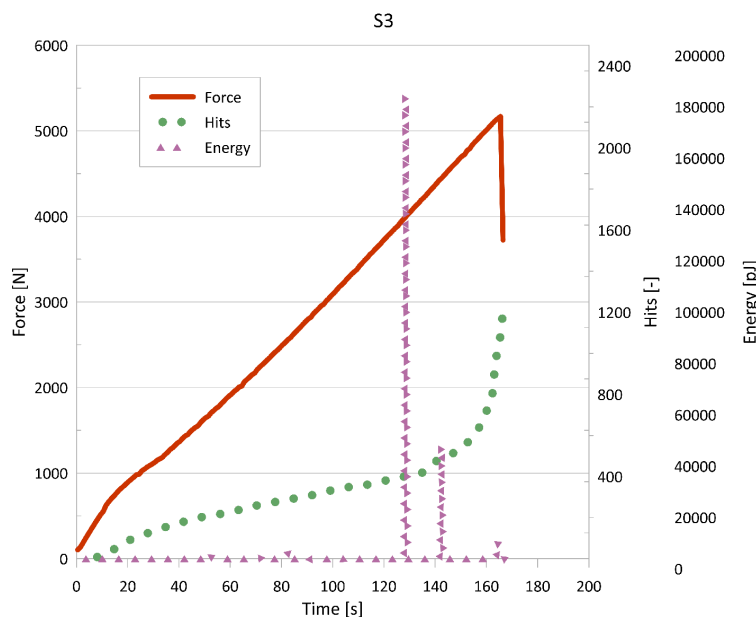


Figure 11. Acoustic emission results on the background of the load applied to specimen S3

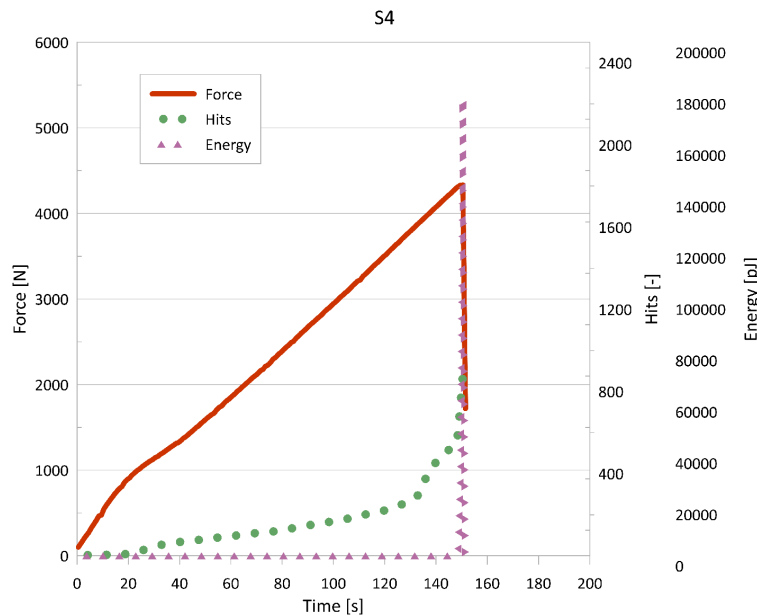


Figure 12. Acoustic emission results on the background of the load applied to specimen S4

CONCLUSIONS

The analysis of the acoustic emission registered during the ENF tests on the composite beams was performed. Application of the acoustic emission sensors has been used from the point of view of more precise determination of propagation initiation. This method detected and monitored deforms under stress, and then analyze the results and describe a materials condition and locate any defects.

Experimental research confirmed proper use of FFT analysis of the raw AE signal to describe damage phenomena, including standard parameters, such as the hits, the counts, the energy and the amplitude. The obtained quantities allow classification of signals, and thus of destructive processes. The more EA parameters recorded, the more accurate the process identification, but the more difficult and labor-intensive is the classification. The research revealed both the types and the sequence of the defects occurring in the composite material during loading. The analysis of the effect of the interface fiber angles mismatch was also provided. In Addition, the similarities and discrepancies of the AE results obtained for similar specimens were discussed. Further studies supported with the fractographic observations of the delamination interfaces and a sophisticated wavelet analysis of the AE data are planned. A more detailed analysis of the issues described above is currently underway and will be described in the next extensive article.

Acknowledgements

The paper was financially supported by the Ministerial Research Project No. DEC-2016/21/B/ST8/03160 financed by the Polish National Science Centre.

REFERENCES

1. Wyslowski P., Debski H., Rozylo P., Falkowicz K. A study of stability and post-critical behaviour of thin walled composite profiles under compression. *Eksploracja i Niezawodność – Maintenance and Reliability* 2016; 18(4): 632–637.
2. de Moraes A.B., de Moura M.F.S.F. Evaluation of initiation criteria used in interlaminar fracture tests. *Engineering Fracture Mechanics* 2006; 73: 2264–2276.
3. AMSY-5 User Manual, 2009.
4. Kubiak T. et al. Experimental investigation of failure process in compressed channel-section GFRP laminate columns assisted with the acoustic emission method. *Composite Structures* 2015; 133: 921–929.
5. Rusinek R. et al. Dynamics of the middle ear ossicles with an SMA prosthesis. *International Journal of Mechanical Sciences* 2017; 127: 163–175.
6. Wevers M. *NDT&E International* 1997; 30 (2): 99–106.
7. Bhat M., Majeed M., Murthy C. *NDT&E International* 1994; 27 (1): 27–31.
8. Leone C., Caprino G., de Iorio I. *Composites Science and Technology* 2006; 66: 233–239.

9. Teter A. et al. On buckling collapse and failure analysis of thin-walled composite lipped-channel columns subjected to uniaxial compression, *Thin-Walled Structures* 2014; 85: 324–331.
10. Arumugam V. et al. Ultimate Strength Prediction of Carbon/Epoxy Tensile Specimens from Acoustic Emission Data. *J. Mater. Sci. Technol.*, 2010; 26(8): 725–772.
11. Scholey J.J. et al. Quantitative experimental measurements of matrix cracking and delamination using acoustic emission. *Composites* 2010; A(41): 612–623.
12. Pereira A.B., de Morais A.B. Mixed mode I + II interlaminar fracture of carbon/epoxy laminates. *Composites* 2008; A39(2): 322–333.
13. Kłonica M. et al. Polyamide 6 surface layer following ozone treatment. *International Journal of Adhesion and Adhesives* 2016; 64: 179–187.
14. Oskouei A.R. et al. An integrated approach based on acoustic emission and mechanical information to evaluate the delamination fracture toughness at mode I in composite laminate. *Materials and Design* 2011; 32: 1444–1455.
15. Samborski S. Numerical analysis of the DCB test configuration applicability to mechanically coupled Fiber Reinforced Laminated Composite beams. *Composite Structures* 2016; 152: 477–487.
16. Brunner A.J. et al. A status report on delamination resistance testing of polymer–matrix composites. *Engineering Fracture Mechanics* 2008; 75: 2779–2794.
17. Cooley J.W., Tukey J.W. An Algorithm for the Machine Calculation of Complex Fourier Series. *Math. Comput.*, 1965; 19:2: 97–301
18. ASTM D7905 Standard.
19. Samborski S. Analysis of the end-notched flexure test configuration applicability for mechanically coupled fiber reinforced composite laminates. *Composite Structures* 2017; 163: 342–349.
20. Ducept F. et al. An experimental study to validate tests used to determine mixed mode failure criteria of glass/epoxy composites. *Composites* 1997; 28A: 719–729.
21. Ni Q.-Q., Jinen E. Fracture Behavior And Acoustic Emission In Bending Tests On Single-Fiber Composites. *Engineering Fracture Mechanics* 1997; 56(6): 779–796.
22. Benmedakhene S. et al. Initiation and growth of delamination in glass/epoxy composites subjected to static and dynamic loading by acoustic emission monitoring. *Compos Sci Technol* 1999; 59: 201–208.
23. Bieniaś J., Dadej K., Surowska B. Interlaminar fracture toughness of glass and carbon reinforced multidirectional fiber metal laminates. *Engineering Fracture Mechanics* 2017; 175: 127–145
24. Debski H. et al. Local buckling, post-buckling and collapse of thin-walled channel section composite columns subjected to quasi-static compression. *Composite Structures* 2016; 136: 593–601.